Entropic Attraction of Polymers toward Surfaces and Its Relationship to Surface Tension

Venkatachala S. Minnikanti and Lynden A. Archer*

School of Chemical and Biomolecular Engineering, Cornell University, Ithaca, New York 14853

Received June 20, 2006; Revised Manuscript Received August 30, 2006

ABSTRACT: Experimental methods for estimating entropic attraction parameters, U^e (attraction of chain ends) and U^j (repulsion of branched points), are important for quantifying surface enrichment of arbitrarily branched polymer components in blends. Measurements of U^e and U^j are also important for determining points of reversal of enrichment, where a small linear or branched species with higher surface energy is preferentially enriched at the surface of a blend with a chemically different, yet miscible polymer. In this article, we show that measurements of polymer surface tension as a function of molecular weight provides a simple tool for quantifying their entropic attraction to surfaces. Specifically, we show that in the limit of high molar mass the surface tension γ of a branched polymer with n_e ends and n_j branch points varies as $\gamma|_{M_w} \cong \gamma|_\infty + [\rho_b RT(n_e U^e + n_j U^j)]/M_w$, where M_w is the molecular weight of the polymer, ρ_b is the bulk density, R is the gas constant, and T is the temperature. Surface tension values predicted using this expression are compared with values determined from self-consistent-field theory simulations of polymers on a lattice, including compressibility effects. We also estimate the value of U^e from published surface tension data for polystyrene and use the estimate to predict surface enrichment in linear polystyrene/deuterated polystyrene blends. Significantly, we find that the phenomenon of reversal of isotopic enrichment at PS/dPS blend surfaces reported by Hariharan et al. [*J. Chem. Phys.* **1993**, *98*, 4163−4173] is quite well predicted using the linear response theory.

1. Introduction

Selective migration of oligomer and polymeric additives toward the surface of a host polymer is important for scientific as well as practical reasons. Understanding this phenomenon is an essential first step in any effort to design additives/plasticizers that do not bloom to polymer surfaces. Theories capable of predicting the direction and magnitude of surface migration can be exploited, for example, to devise methods for functionalizing polymer surfaces with surface specific additives. In multicomponent polymer blends, the species having the lower cohesive energy density is normally enriched at the surface.[1−6] As the number of chain ends is increased, however, entropic factors or end effects can become comparable to the usual energetic driving forces to determine the surface composition. Additives with branched structures such as combs, multiarm stars, and dendrimers are therefore attractive for polymer surface modification not only because they provide a large numbers of chain ends that can be decorated with specific chemistries but also because the entropic attraction of these species to surfaces is anticipated to be large. A heretofore unresolved question concerns the way this end−surface attraction can be estimated from simple experimental data.

Walton and Mayes[7] used numerical self-consistent-field theory calculations to show that there exists a critical molecular weight below which an energetically unfavorable branched polymer is always enriched at the surface of a linear host when energetic and entropic factors are considered. In a recent study, Foster and co-workers used isotopically labeled branched polystyrene molecules in linear polystyrene hosts to characterize the effect of molecular architecture on surface migration.[8] However, even isotopic substitution introduces energetic effects that prevent straightforward interpretation of their experimental results. Minnikanti and Archer recently developed a linear response theory that accounts for the energetic and entropic driving forces that govern surface enrichment of branched and linear additives in polymer hosts.[6] This analysis produces a simple analytical expression for the crossover molecular weight in linear/linear and branched/linear polymer blends. Specifically, the authors showed that the critical molecular weight or degree of polymerization, N_B^c, of a branched species below which even an energetically unfavorable branched polymer additive is always enriched at the surface of a branched/linear blend is given by

$$N_B^c = -\frac{(n_e U_B{}^e + n_j U_B{}^j)/\Delta U_B{}^s}{1 - 2U_L{}^e/(N_L \Delta U_B{}^s)} \tag{1}$$

Here, N_L is the degree of polymerization of the linear species, n_e is the total number of ends, and n_j the number of branch points, defined as a point where more than two polymer segments meet, of a arbitrary branched additive. $\Delta U_B{}^s$ is the integrated strength of relative attraction of segments of branched species toward the surface. It represents the difference in potentials acting on the midsections of branched species and the linear polymer host due to loss of coordination number at the surface. $U_B{}^e$ and $U_B{}^j$ represent the integrated strength of attraction of the end and branched point, respectively, of the branched polymer toward the surface. $U_L{}^e$ is the corresponding integrated strength of attraction of the ends of the linear host polymer. $\Delta U_B{}^s$, $U_B{}^e$, $U_L{}^e$, and $U_B{}^j$ are measured in the units of length. When the ends of a polymer are chemically identical to the midsections, $U^e$and U^j reflect the entropic interactions between polymers and the surface. In practical applications, however, the ends of a polymer are rarely chemically the same as the midsections, implying that U^e will also generally reflect energetic contributions as well. This situation partially stems from the fact that the initiator and terminating species used for large-scale polymer synthesis are typically chemically different

* Corresponding author. E-mail: laa25@cornell.edu.

10.1021/ma061377d CCC: $33.50
Published on Web 09/30/2006

from the monomer. It is therefore apparent that quantitative analysis of the reversal of enrichment phenomena requires independent estimates for the parameters $\Delta U_B{}^s$, $U_B{}^e$, $U_B{}^j$, and $U_L{}^e$.

Sometime ago, Hariharan, Kumar, and Russell measured the composition of deuterated linear polystyrene (dPS) in binary blends with linear polystyrene (PS).[2] They observed that below a critical PS molecular weight PS is preferentially enriched at the blend surface. Because of the slightly lower cohesive energy density of dPS compared to PS, energetic factors favor the deuterated species at the surface.[1−6] Substituting $n_e = 2$ and $n_j = 0$ in eq 1 yields $N_h{}^c = (2U^e/\Delta U_d{}^s)/[1 + 2U^e/(N_d\Delta U_d{}^s)]$, where "*d*" represents the energetically preferred but higher molecular weight species (dPS in ref 2) and "*h*" the lower molecular weight polymer. Equation 1 therefore provides a simple explanation for the crossover phenomenon, but quantitative comparisons require independent knowledge of $\Delta U_d{}^s$ and U^e.

$\Delta U_d{}^s$ is related to the difference in surface tensions and Flory−Huggins χ parameter of interaction[9] and can be obtained experimentally.[3−5,9−12] It is the integrated strength of relative attraction of segments of deuterated species toward the surface. U^e, on the other hand, is generally difficult to obtain, particularly when entropic factors are important. In this paper we explore a procedure for estimating these parameters from pure component surface tension data. We will show that the initial slope of surface tension as a function of inverse molecular weight provides a simple way to extract U^e for linear polymers. Self-consistent-field theory calculations based on the formulation of Scheutjens and Fleer[13] will be used as a framework to develop the theoretical model and also to estimate the errors inherent in the theoretical formulation. Finally, we will use the U^e estimate for linear PS to predict the crossover molecular weight and other features of the surface enrichment data reported by Hariharan et al.[2]

To begin, we will develop the procedure for extracting the parameters $U_B{}^e$, $U_B{}^j$, and $U_L{}^e$ for an incompressible polymer melt. Later we will extend the formulation to a more realistic, compressible polymer melt to capture the effect of density gradients near the surface.

2. Incompressible Polymer Systems

2.1. Surface Tension Dependence on Molecular Weight. Consider a melt of an incompressible polymer of degree of polymerization N on a semiinfinite cubic lattice (also refer to refs 6 and 16). The lattice spacing is taken to be l, and each polymer segment occupies one lattice site. The next segment of the polymer can occupy anyone of the z (= 6 as in a cubic lattice) coordination sites that surround the lattice site occupied by the previous segment. The layer zero represents a hard neutral wall signifying a polymer−vacuum/air interface. Let there be L lattice sites per lattice layer and let lattice layer M be a layer deep within the polymer bulk where the effect of the hard wall/interface is no longer felt. A hard neutral wall will not have any energy of interaction with polymer segments in layer one. For an ideal polymer gas composed of noninteracting segments, the entropic confinement effect of the wall should therefore reduce the density of a polymer near the surface. For an incompressible polymer melt, however, the density is by definition constant in all lattice layers, implying that to simultaneously capture the effect of the wall and maintain incompressibility, incompressibility/space-filling potentials must act on polymer segments in lattice layers near the wall. These potentials are related to the Lagrangian parameters that are introduced while minimizing the partition function under the constraint of constant density across all the lattice layers in the polymer melt. Within the framework of Scheutjens and Fleer, the surface tension γ of the incompressible lattice polymer may therefore be expressed as[13]

$$\frac{\gamma a_s}{k_B T}\Big|_N = \frac{\gamma_m a_s}{k_B T} - \sum_{i=1}^{\infty}\alpha_i \tag{2}$$

where a_s is related to the area of each lattice site. It is equal to υ_s/l, where υ_s is the segmental volume, which need not be equal to l^3 the volume of each lattice site. k_B is the Boltzmann constant, and T is the thermodynamic temperature of the system. α_i is the incompressibility/space-filling potential, in units of k_BT, acting on any segment of the polymer in lattice layer i. γ_m is the contribution to the surface tension due missing neighbors at the surface and is independent of the molecular weight of the polymer. Therefore, any dependence of the surface tension on degree of polymerization N can only come from the second term in eq 2, i.e., the sum of the space-filling potentials acting across all the lattice sites. Our goal is to obtain an analytical relationship between the surface tension of the polymer and its degree of polymerization.

We will attempt to derive an asymptotic form of surface tension in the limit of large polymer molecular weights, i.e., the so-called infinite molecular weight limit. Let the incompressibility potential acting in any layer i be denoted by $\alpha_i{}^\infty$ and perturbations due to the finite polymer molecular weight be denoted by $\Delta\alpha_i{}^N$. On this basis eq 2 can be rewritten as

$$\frac{\gamma a_s}{k_B T}\Big|_r = \frac{\gamma_m a_s}{k_B T} - \sum_{i=1}^{\infty}(\alpha_i{}^\infty + \Delta\alpha_i{}^N) = \frac{\gamma a_s}{k_B T}\Big|_\infty - \sum_{i=1}^{\infty}\Delta\alpha_i{}^N \tag{3}$$

where the term $\Delta\alpha_i{}^N$ strictly represents the change to the incompressibility field due to the presence of chain ends; i.e., it reflects the fact that chain ends are entropically attracted toward the surface.[6,14−16] This end−surface attraction contributes to $\Delta\alpha_i{}^N$'s terms in the incompressibility field acting on all polymer segments near the surface to maintain the incompressibility constraint.

Perturbations in incompressibility field due to the presence of chain ends near a surface can be deduced by recourse to the random phase approximation.[17,18] Consider a melt of an incompressible pure component linear, N-mer, chain in three-dimensional space, unrestricted by any presence of a wall. Suppose a field acts only on the ends of this polymer. Changes to the incompressibility field required to maintain the constraint of incompressibility as a result of applying the field on the ends of the polymer can be computed as follows. Let $S^{ss}[\vec{r},\vec{r}']$ and $S^{se}[\vec{r},\vec{r}']$ be the ideal Gaussian free polymer segment−segment and segment−end correlation functions, respectively. Changes to the mean density at any point in space due to the presence of the incompressibility field and the imposed field acting on the ends of the polymer can be written as

$$\psi[\vec{r}] = -\int \mathrm{d}r'\, S^{ss}[\vec{r},\vec{r}']\Delta\alpha^N[\vec{r}'] - \int \mathrm{d}r'\, S^{se}[\vec{r},\vec{r}']u^e[\vec{r}'] \tag{4}$$

where $\psi[\vec{r}] = \langle r[\vec{r}] - \rho_b\rangle$ is the mean of the changes to the bulk density ρ_b at any point in space. $u^e[\vec{r}']$ is the perturbing field imposed on the ends of the polymer at any point in space $\vec{r}'$ in space also in the units of k_BT. The incompressibility criterion is satisfied when $\psi[\vec{r}] = 0$. We can solve for the unique incompressibility field, $\Delta\alpha^N[\vec{r}']$, for any given field $u^e[\vec{r}']$ acting on the ends of the polymer, which is required to maintain the

criterion for incompressibility. Substituting $\psi[\vec{r}] = 0$ in eq 4 and taking the Fourier transform of the resultant expression yields

$$\Delta\tilde{\alpha}^N[q] = -\frac{\tilde{S}^{se}[q]u^e[q]}{\tilde{S}^{ss}[q]} \tag{5}$$

Equation 5 is evidently a general expression valid for any spatial distribution of the imposed perturbing field acting on the chain ends. We now consider a special case when the perturbing field $u^e[\vec{r}]$ is acting only on a two-dimensional infinite flat plane. That is, we divide the free space into two halves and take the dividing plane to be $x = 0$, which passes through the origin. The perturbing field is constant and is of the form of a Dirac delta in the dimension x and exists only in the dividing plane just described. We can now adapt the solution for this particular case to a polymer near a surface, using the reflecting boundary condition.[6,14−16] Dirac delta-like potentials for the entropic attraction of chain ends to the surface are justified because the interaction is localized in a small region near the surface, compared to the radius of gyration of the polymer. The polymer density changes from the bulk value to zero in this same region. The length scale on which this change occurs is the Edwards correlation length,[14−17] which is of the order of Kuhn length of the polymer. And for incompressible lattice polymers, this region is typically of the size of first few lattice layers near the wall[6] (1−2 layers). Because of the reflecting symmetry at a surface, the problem of finding the solution to responses in the bulk is similar to the half space problem of finding the responses to half the amount of perturbing potentials acting at the wall. Therefore, we take $u^e[x] = 2U^e\delta[0]$, where U^e is the integrated strength of attraction of the ends toward the surface and $\delta[0]$ is the Dirac delta function at $x = 0$. The factor 2 is a result of even extension of the perturbing field into the image space. The integral of the changes in the incompressibility field due to the ends near the surface can then be simply obtained by taking $q = 0$ and retaining half of the resultant expression

$$\int_0^\infty dz\, \Delta\alpha^N[z] = -\frac{2U^e}{N} \cong l\sum_1^\infty \Delta\alpha_i^N \tag{6}$$

In the above expression we have used the identity[6,15] $\tilde{S}^{se}[q=0] = 2\rho_b$ and $\tilde{S}^{ss}[q=0] = N\rho_b$. Substituting in eq 3 the surface tension should depend on the degree of polymerization for high molar mass polymers as

$$\frac{\gamma a_s}{k_BT}\Big|_N \cong \frac{\gamma a_s}{k_BT}\Big|_\infty + \frac{2U^e/l}{N} \tag{7}$$

The above analysis can be readily extended to branched polymers. Specifically, if the appropriate correlation functions for a branched polymer are properly introduced in eq 5, it is straightforward to show that

$$\int_0^\infty dz\, \Delta\alpha^N[z] = -\frac{(n_eU^e + n_jU^j)}{N} \cong l\sum_1^\infty \Delta\alpha_i^N \tag{8}$$

where U^j is the integrated strength of attraction of the branched point toward the surface (which depends on the number of arms meeting at the branched point). n_e and n_j are the number of ends and branched points of the branched polymer. Substituting this result in eq 3 now yields

$$\frac{\gamma a_s}{k_BT}\Big|_N \cong \frac{\gamma a_s}{k_BT}\Big|_\infty + \frac{(n_eU^e + n_jU^j)/l}{N} \tag{9}$$

The above derivation can be extended to terms $O[1/N^2]$ and higher by including higher order correlation terms in eq 4. However, in this work we will focus on high molecular weight polymers, for which the $O[1/N]$ terms are sufficient. To validate the approximate analytical expressions summarized in eqs 7 and 9, it is useful to compare their predictions with results from incompressible polymer lattice simulations.

2.2. Comparison with Incompressible Lattice Simulations. We focus on a single polymer species (symmetric star and linear) on a semiinfinite lattice. Let layer 1 be the layer next to the layer describing vacuum/hard neutral wall and let lattice layer M be a layer deep inside the bulk of the polymer such that the effect of the wall is no longer felt. Now let λ_1 be the fraction of lattice sites surrounding a particular lattice site in the adjacent lattice layer and λ_0 be the fraction of surrounding lattice sites belonging to the same lattice layer. On a cubic lattice of coordination number 6, λ_1 then takes a value of 1/6 and λ_0 takes a value of 2/3. As there are two neighboring layers for each lattice point therefore we have the identity $\lambda_0 + 2\lambda_1 = 1$. On such a lattice a self-consistent potential

$$u[i] = 1/N + \alpha'[i] + \delta_{1,i}\chi_s = \alpha[i] + \delta_{1,i}\chi_s \tag{10}$$

acts on all segments of the polymer in any lattice layer[13] i. Here, $\alpha'[i]$ is the Lagrangian parameter used to maintain the criterion of incompressibility in any lattice layer. For the case of a single component melt, it is related to the incompressibility potential as[6,13] $\alpha[i] = 1/N + \alpha'[i]$. Since there is only one species involved in these simulations, these potentials are purely space filling in lattice layers numbered greater than one. $\delta_{1,i}$ is the Kronecker delta, and χ_s is the additional potential felt by polymer segments in lattice layer 1, adjacent to the wall. For the case of a hard neutral wall, this contribution comes from the effect of missing neighbors. The surface tension can be calculated from the values of the converged self-consistent potentials determined from simulations with the expression[13]

$$\frac{\gamma a_s}{k_BT}\Big|_N = \chi_s - \sum_{i=1}^\infty \alpha[i]$$

When compared with eq 2, χ_s can be identified with the term $\gamma_m a_s/k_BT$, which represents the energetic contribution to the surface tension.[13] The parameter χ_s contributes a constant, molecular-weight-independent term to the surface tension. Therefore, the difference of surface tensions between an infinite molecular weight and finite molecular weight polymer, $(\gamma a_s/k_BT)|_N - (\gamma a_s/k_BT)|_\infty$, is independent of the term χ_s. This makes it possible to set χ_s to zero in our simulations without incident. To ensure the continuity of discussion, further elaboration of the simulation scheme is left to Appendix A. To compute the surface tension of an infinitely long polymer, a steady-state equation for the propagators is used (also elaborated in Appendix A). The self-consistent potentials so obtained may then be used to calculate the surface tension. This analysis yields $(\gamma a_s/k_BT)|_\infty = 0.1842$ in nondimensional units.

Figure 1 summarizes the difference in surface tension of a finite and infinitely long linear and star-branched polymers, $[(\gamma_N - \gamma_\infty)a_s]/k_BT$, as a function of inverse total degree of polymerization $1/N$. Symbols represent the simulation results and lines are the predictions from eqs 7 and 9. Values for the entropic attractions of ends U^e and repulsion of a p-arm branch point

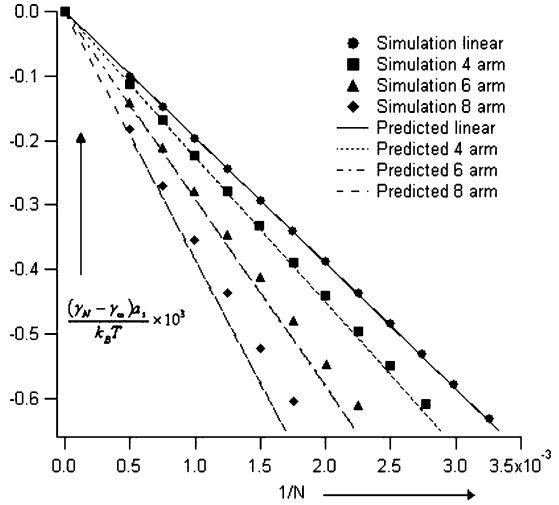

Figure 1. Variation of surface tension with inverse degree of polymerization N of polymers of various architectures in an incompressible lattice framework. The filled symbols represent the predictions of lattice simulations, and the lines correspond to the predictions based on eqs 7 and 9.

Table 1. Attraction of Ends and Repulsion of Joints of Polymers toward Surfaces[a]

moieties	variable	value in lattice units (l), **A**	value in lattice units (l^*), **B**
end	U^e	−0.0975	−0.3791
4-arm joint	U_4^j	0.1645	0.3503
6-arm joint	U_6^j	0.2945	0.5571
8-arm joint	U_8^j	0.3963	0.7044

[a] Incompressible (**A**) and compressible (**B**) lattice simulations at the conditions of the simulation.

Table 2. Anticipated and Measured Initial Slopes for Incompressible Polymer Simulations of Surface Tension

obtained initial slope	anticipated initial slope	percentage diff (%)
$m_{\text{linear}}^{N=\infty} = -0.1999$	$2U^e/l = -0.1951$	−2.41
$m_{4-\text{arm}}^{N=\infty} = -0.2274$	$(4U^e + U_4^j)/l = -0.2256$	−0.79
$m_{6-\text{arm}}^{N=\infty} = -0.2848$	$(6U^e + U_6^j)/l = -0.2907$	+2.07
$m_{8-\text{arm}}^{N=\infty} = -0.3650$	$(8U^e + U_8^j)/l = -0.3840$	+5.19

U_p^j toward the surface have been calculated previously[16] and are listed in Table 1. It is immediately apparent from Figure 1 that for high molecular weight polymers the theoretical predictions are in good to excellent accord with results from self-consistent-field simulations, irrespective of polymer architecture. More detailed comparisons of the slopes of the simulated and theoretical surface tension plots are provided in Table 2. The initial slopes in the limit of infinite molecular weight obtained from the simulations were obtained by drawing a line between the point corresponding to infinite molecular weight (obtained from ground state simulations) and the largest molecular weight polymer simulated for the corresponding architecture. The difference between the obtained slopes and predicted ones is also observed to become progressively smaller as the polymer molecular weights are increased. We observe that the difference between the predictions of surface tension and the observed simulation data increase progressively as the molecular weights of the polymers are reduced. This trend is seen in all cases whether the polymer is linear or branched. Additionally, we observe that for any particular molecular weight the deviation between the predicted and observed surface tensions increases as the degree of branching increases. We have identified two possible sources for this behavior.

First, the analytical response theory assumes that the pseudo-entropic potentials acting on the ends and the joints of a branched polymer are of the form of Dirac delta functions acting at the origin. This effectively coarse grains the surface interactions over the small depletion region near the surface (or the first few lattice layers in an incompressible lattice). This analysis is therefore most accurate when the size of the polymer (R_g) is much larger than the depletion region at the surface (or many times larger than a lattice size in incompressible lattice simulations[16]). Significant deviations are expected in analyses of small molecular weight stars or linear polymers, where R_g is comparable to the depletion region thickness. The errors are also expected to be greater for an equal molecular weight star compared to that of the linear. For example, the radius of gyration of the 569-segment 8-arm star considered in the paper is just 5.6 lattice units, while for the equivalent molecular weight linear polymer R_g is 9.7 lattice units. Hence, the greater deviation from theory observed for the 8-arm star is consistent with this reasoning.

Another, perhaps more obvious source of error arises from higher order terms in the response equation. Specifically, according to the response theory the surface tension depends on polymer molecular weight as $\gamma|_{M_w} \cong \gamma|_\infty + [(\rho_b RT(n_e U^e + n_j U^j)]/M_w$. This expression is a thermodynamic identity within the random phase approximation when higher order terms are included. This means that in reality there is an infinite series in powers of $1/M_w$ on the right-hand side of eqs 7 and 9. Truncating the series at the first term means that the expression will lead to progressively larger errors as the polymer molecular weight is lowered. Work is already underway to extend these expressions to higher order in $1/M_w$.

In closing, it should nonetheless be noted that the surface tension dependence on molecular weight predicted by eq 7 is consistent with the empirical form reported by Theodorou,[19] $(\gamma a_s/k_BT)|_N = 0.184(1 - 1/N)$. Specifically, on substituting values for surface tension of an infinitely long polymer and the attraction of ends from Table 2, the surface tension of a linear polymer on a lattice is predicted to be $(\gamma a_s/k_BT)|_N = 0.184 - 0.195/N = 0.184(1 - 1.06/N)$, which is very close to Theodorou's result.

3. Compressible Polymer Systems

3.1. Surface Tension Dependence on Molecular Weight. Kumar and Jones[20,21] have shown that the surface tension dependence on molecular weight of real, compressible polymers has additional contributions due to density gradients at the surface. In our earlier publication,[16] we showed that, but for a small depletion layer near the surface, polymers simulated in the compressible lattice framework behave almost exactly like incompressible polymers near a surface. This difference effectively increases the magnitude of entropic attraction of the ends of the polymer (and entropic repulsion of the branched points) to the surface. It follows that by appropriately modifying the attractions of ends and repulsion of joints the analysis leading up to eqs 7 and 9 can be extended to describe surface tension of compressible polymer systems.

To account for compressibility effects, one typically introduces empty voids as solvent.[16,22−24] The volume fraction of voids and polymer are then calculated at bulk conditions through use of an appropriate equation of state. A lattice polymer follows the Sanchez and Lacombe equation of state.[16,25] Under such circumstances the actual volume occupied by a molecule of a polymer would be smaller than that considered in incompressible lattice polymer assumption, to make room for the voids. If v_s^*

is the hard core volume of a segment of polymer excluding the void space and N^* is some equivalent degree of polymerization of the polymer, then we can make a comparison with the incompressible model and the compressible one. We can take $(N^*v_s^*)/(Nv_s) = \varphi_b$, the volume fraction of the polymer in bulk. Here N and v_s are the degree of polymerization and volume of a segment in the incompressible case. N^* could be taken equal to that of N, but to preserve generality we assume they are different. The invariant in these two models is the radius of gyration/statistical end-to-end distance of the polymer, which leads to another relationship, $N^*(l^*)^2 = N(l)^2$ where l and l^* are the lattice spacing chosen in the compressible and incompressible systems, respectively. Thus, the area $a_s^* = v_s^*/l^*$ which nondimensionalizes the surface tension is related to the area a_s used in the incompressible model as $a_s/a_s^* = (1/\varphi_b)(l/l^*)$. Substituting for a_s in the incompressible model, we obtain the equivalent surface tension relationships in the compressible model for linear and branched polymers, respectively

$$\frac{\gamma a_s^*}{k_B T}|_{N^*} \cong \frac{\gamma a_s^*}{k_B T}|_\infty + \frac{\varphi_b(2U^e/l^*)}{N^*} \tag{11}$$

$$\frac{\gamma a_s^*}{k_B T}|_{N} = \frac{\gamma a_s^*}{k_B T}|_\infty + \frac{\varphi_b(n_e U^e + n_j U^j)/l^*}{N^*} \tag{12}$$

3.2. Comparison with Compressible Lattice Simulations. We will compare the predictions of eqs 11 and 12 with computer simulations of a polymer on a semiinfinite lattice, including compressibility effects. Compressibility is taken into account by including voids in the lattice. The presence of voids in the polymer melt eliminate the Lagrangian parameters introduced earlier to maintain the space-filling constraint, making it also possible to maintain density gradients near an interface. The surface tension can therefore be written as follows:[13]

$$\frac{\gamma a_s^*}{k_B T}|_{N^*} = \sum_{i=1}^{\infty}\left[\left(1 - \frac{1}{N^*}\right)(\varphi[i] - \varphi_b) + \ln\left[\frac{1-\varphi[i]}{1-\varphi_b}\right] + \chi_v(\varphi[i]\langle\varphi[i]\rangle - \varphi_b^2)\right] \tag{13}$$

Here, $\varphi[i]$ is the volume fraction of polymer segments in the lattice layer i. The variable $\langle\varphi[i]\rangle = \lambda_1\varphi[i+1] + \lambda_0\varphi[i] + \lambda_1\varphi[i-1]$ represents the average volume fraction of segments surrounding a particular lattice site in layer i. χ_v is the Flory−Huggins interaction parameter between the polymer segments and voids. To ensure the continuity of discussion, further elaboration of the simulation scheme is provided in Appendix B.

We will simulate a polystyrene-like material at a temperature of $T = 450$ K and pressure $P = 0$ MPa. Polystyrene has a characteristic temperature $T^* = 735$ K and a characteristic pressure of pressure $P^* = 358$ MPa.[26] The Flory−Huggins parameter of interaction between the voids and the polymer segments is related to the temperature of the system and characteristic temperature as[16,22,23] $\chi_v = T^*/T$. At the given pressure and temperature, the bulk volume fraction φ_b of polymer segments is obtained by solving the Sanchez−Lacombe equation of state:[16,22,25,26]

$$\varphi_b^2 + \frac{P}{P^*} + \frac{T}{T^*}\left[\ln[1-\varphi_b] + \left(1 - \frac{1}{N^*}\right)\varphi_b\right] = 0 \tag{14}$$

This expression is taken to be the same for linear and branched molecules with the same overall degree of polymerization, N^*. For densely branched polymers, some conformations may be restricted near the branch point, and the contribution of the entropic term to the free energy will not be the same as for a linear polymer. However, such effects are not considered here.

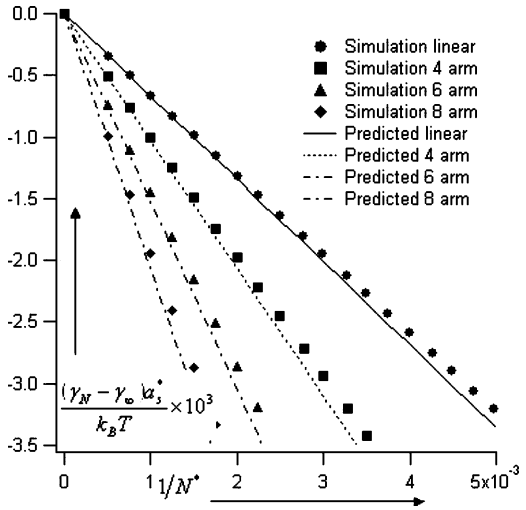

Figure 2. Variation of surface tension with inverse degree of polymerization N^* of polymers of various architectures in a compressible lattice framework. The filled symbols represent the predictions of lattice simulations, and the lines correspond to the predictions based on eqs 7 and 9.

The self-consistent potentials and volume fractions of polymer segments in various lattice layers are determined from converged simulations. Insertion of the converged self-consistent volume fractions into eq 13 allows the surface tension of the polymer to be computed. For the surface tension of an infinitely long polymer the volume fractions are determined by using the corresponding steady-state equation for the propagators, which is explained in Appendix B. At the conditions of the simulation, the dimensionless surface tension of the infinitely long compressible polymer is found to be equal to $(\gamma a_s^*/k_B T)|_\infty = 0.2827$. The difference in surface tension of polymers with finite and infinite degree of polymerization, $[(\gamma_{N^*} - \gamma_\infty)a_s^*]/k_B T$, is plotted as a function of inverse degree of polymerization $1/N^*$ in Figure 2. Again, the simulated values (symbols) for linear and various symmetric star polymers are compared with theoretical surface tension predictions (lines) obtained using eqs 11 and 12. As was the case for the incompressible polymer model, the slopes of these plots are seen to become progressively steeper for stars with greater number of arms.

For the compressible lattice polymer model, using ground-state calculations the entropic attractions of ends and repulsions of the branched points toward the surface can be calculated at the conditions of the simulation,[16] and the values are listed in Table 1. Notice that the predicted surface tension from eqs 11 and 12 contain the bulk volume fraction term φ_b, which depends on the degree of polymerization through the equation of state (eq 14). This equation of state can be written in the form of a Taylor expansion about the volume fraction at infinite degree of polymerization as

$$\varphi_b = \varphi_b^\infty + \frac{T/T^*}{2 - (T/T^*)/(1-\varphi_b^\infty)}\frac{1}{N^*} + O\left[\frac{1}{N^{*2}}\right] \tag{15}$$

Here, φ_b^∞ is the bulk volume fraction for an infinitely long polymer. Under the conditions of our simulations φ_b^∞ is evaluated by solving eq 14 in the infinite molecular weight limit, which gives $\varphi_b^\infty = 0.8853$. Thus, in the limit of infinite degree

Table 3. Anticipated Initial Slope and Obtained Initial Slope for Compressible Polymer Simulations of Surface Tension

obtained initial slope	anticipated initial slope	percentage diff (%)
$m_{\text{linear}}^{N=\infty} = -0.6751$	$\varphi_b 2U^e/l^* = -0.6712$	−0.58
$m_{4-\text{arm}}^{N=\infty} = -1.0204$	$\varphi_b(4U^e + U_4^j)/l^* = -1.0324$	+1.17
$m_{6-\text{arm}}^{N=\infty} = -1.4803$	$\varphi_b(6U^e + U_6^j)/l^* = -1.5205$	+2.72
$m_{8-\text{arm}}^{N=\infty} = -1.9817$	$\varphi_b(8U^e + U_8^j)/l^* = -2.0613$	+4.02

of polymerization, the volume fraction of the lattice polymer varies as

$$\varphi_b = 0.8853 - 0.1834\frac{1}{N^*} + O\left[\frac{1}{N^{*2}}\right] \qquad (16)$$

We observe that the term of the order of $1/N^*$ in eq 16 contributes a term of the order of $1/N^{*2}$ in eqs 11 and 12. Since our derivation of the surface tension expressions eqs 7 and 9 neglects nonlinear terms $O(1/N^{*2})$ and higher, we will not include these terms in our analysis. As we will see, neglect of these terms introduces negligible errors for large degrees of polymerization.

For a *p*-arm star polymer, the surface tension predicted through eq 12 is given by

$$\left.\frac{\gamma a_s^*}{k_B T}\right|_{N^*} = \left.\frac{\gamma a_s^*}{k_B T}\right|_{\infty} + \frac{\varphi_b(n_e U^e + U_p^j)/l^*}{N^*}$$

It is apparent from Figure 2 for high molecular weights the simulated and theoretical surface tensions are in good accord. Slopes of the surface tension curves deduced from the simulations are compared with the theoretical predictions in Table 3. The initial slopes in the limit of infinite molecular weight are deduced using the same procedure as for the incompressible lattice simulations. It is evident from Table 3 that the theoretical predictions are generally in good agreement with the values deduced from simulations and that the differences become progressively smaller as the polymer molecular weights are increased.

It should be noted that, in addition to the sources of discrepancies between the analytical estimates of surface tension and the values determined from simulations already discussed for incompressible lattice polymers, there are other sources of error for compressible lattice polymers. In particular, there is a new source of error that first emerges at $O[1/N^2]$, which reflects the effect of changes in bulk density on polymer molecular weight. The Sanchez and Lacombe equation of state suggests a molecular weight dependence of bulk volume fraction (see eq 15). In addition, for a compressible polymer the depletion region (which is responsible for the attraction of the ends toward the surface) is around 4−5 lattice layers. This region is larger than the equivalent region responsible for entropic potentials in the incompressible case.[16]

4. Comparison with Surface Enrichment Experiments

Given the success of the response theory in predicting surface tension values from self-consistent lattice simulations of incompressible and compressible polymers, it is of interest to extend the analysis to the more complex problem of surface enrichment in polymer blends. Hariharan, Kumar, and Russell[2] used neutron reflectivity data to quantify surface enrichment of dPS in PS/dPS linear polymer blends at a fixed temperature of 160 °C.

These authors showed that their data can be fitted to an exponential volume fraction profile. Using their fit values of surface composition of dPS, φ_s^d, and the correlation length ζ, we calculated the integrated surface excess of the deuterated species, $z_d^* = \int_0^\infty(\varphi^d[x] - \varphi_b^d) = \zeta(\varphi_s^d - \varphi_b^d)$. Here φ_b^d is the bulk volume fraction of the dPS. Results from this analysis are presented in Figure 3a−e as a function of degree of polymerization of normal polystyrene N_h in the blends. The confidence intervals in these plots were calculated from the experimental error bars of the measured quantities using standard error propagation formulas.[27]

Figure 3a corresponds to data set 1 from the original work, for which the molecular weights of both the deuterated and normal polystyrenes in the blends are the same and the bulk volume fraction of deuterated polystyrene is $\varphi_b^d = 0.41$. Figure 3b corresponds to data set 2 from the original work. In this case the degree of polymerization of deuterated polystyrene was kept constant at $N_d = 4808$, and the average bulk volume fraction of deuterated polystyrene in the blend is $\varphi_b^d = 0.49$. Parts c and d of Figure 3 correspond to $N_d = 1000$ and 4808 and average bulk volume fractions $\varphi_b^d = 0.47$ and 0.65, respectively. These two figures correspond to data sets 4 and 5 from the original work. The final figure (Figure 3e) corresponds to data set 6 from the original work, for which $N_d = 4808$ and $\varphi_b^d = 0.26$. As shown elsewhere, the integrated surface excess predicted using the response theory is given by[6]

$$z_d^* = -\frac{\Delta U_d^s + 2U^e(1/N_d - 1/N_h)}{1/\varphi_b^d N_d + 1/(1-\varphi_b^d)N_h - 2\chi} \qquad (17)$$

Here, χ is the Flory−Huggins interaction parameter between the two species, ΔU_d^s represents the difference of potential that a dPS segment feels at the surface compared to a normal PS segment due to their slight differences in cohesive energy densities, and U^e is the attraction of ends toward the surface. If the linear polymers have two types of ends, such that if they are initiated anionically by *sec*-butyllithium and terminated by some other species, U^e is taken to be as the arithmetic mean value, i.e., $U^e = (U_1^e + U_2^e)/2$. Although eq 17 above has been derived for an incompressible polymer blend, it is equally valid to represent compressible and hence real polymer blends with it. As mentioned earlier, this is because but for a small depletion layer near the surface polymers simulated in the compressible lattice framework behave almost exactly like incompressible polymers near the surface. The only effective difference is the magnitude of entropic attraction of the ends of the polymer (and entropic repulsion of the branched points) to the surface. Any responses theory that properly accounts for these modifications correctly predicts the enrichements.[6,16] Although U^e can in principle be determined from computer simulations, the values obtained are model dependent and the inevitable energetic contributions cannot be rigorously captured. Here we propose instead to utilize molecular-weight-dependent surface tension data from the same polymers to determine U^e.

A value for the Flory−Huggins χ parameter for PS and dPS at 160 °C can be obtained from the work of Bates and Wignall,[28] $\chi = 1.72 \times 10^{-4}$. ΔU_d^s typically depends on the surface volume fraction of species of the blend. However, it was theoretically estimated by Kumar and Russell[1] to be equal to −0.0033 nm at the conditions of their experiment. The value of ΔU_d^s can also be obtained by interpreting the experimental integrated surface excess of high molecular weight or symmetric PS and dPS blends using the Schmidt and Binder theory.[10] Using this approach, Jones and co-workers[3] report $\Delta U_d^s = -0.0024 + 0.00046\varphi_s^d$ nm at 184 °C. Zhao and co-workers[5] later obtained a more general expression, valid for a greater range of values

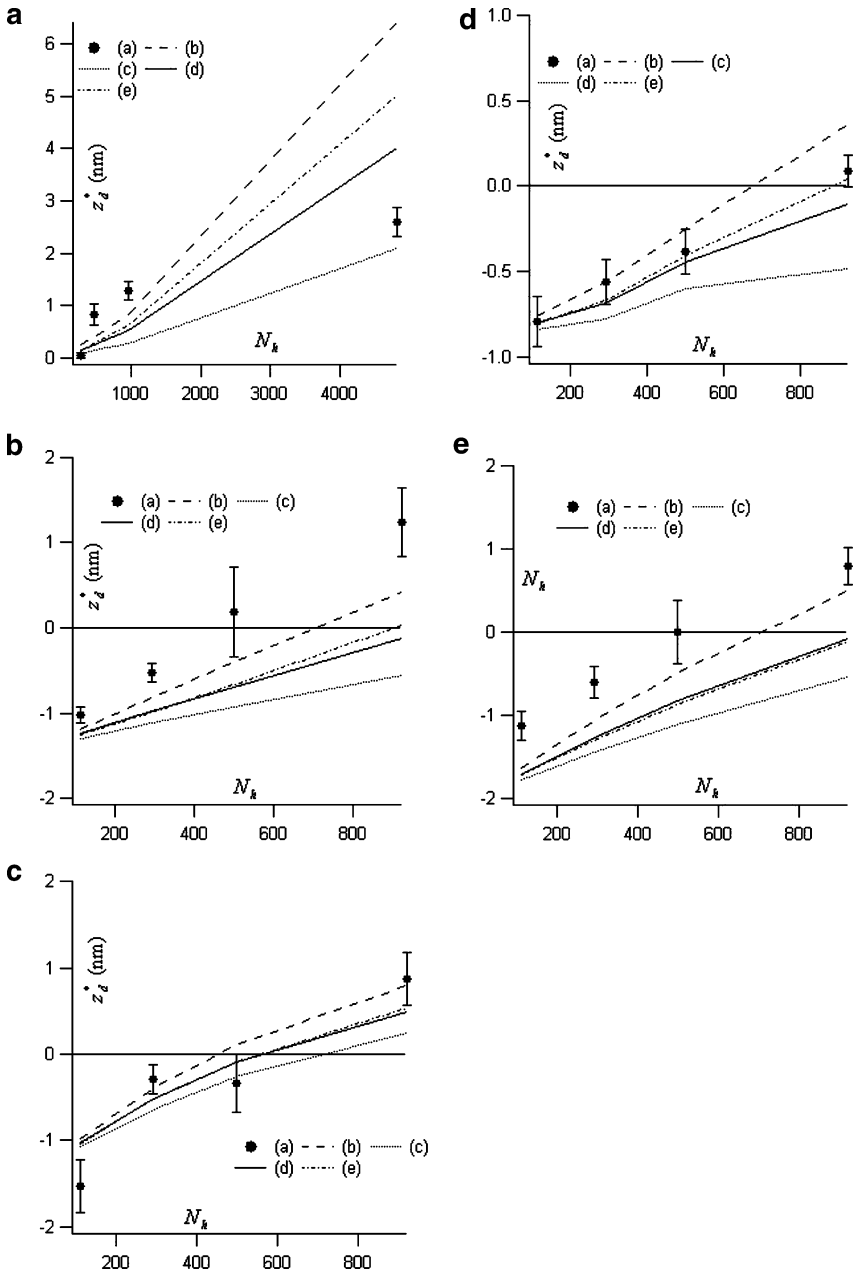

Figure 3. Comparison of integrated surface excess of dPS z_d* as a function of degree of polymerization N_h of PS in blends of PS−dPS from the data of Hariharan, Kumar, and Russell[2] and prediction of the response theory. Parts a, b, c, d, and e correspond to data sets 1, 2, 4, 5, and 6 from the original reference. The symbols (a) represent the experimentally observed excesses. The lines represent the predictions of the response theory (b) for the case when ΔU_d^s is taken from the work of Kumar and Russell,[1] (c) for the case when ΔU_d^s is estimated from the work of Budkowski, Steiner, and Klein,[12] (d) for the case when ΔU_d^s is estimated from the work of Jones and co-workers,[3] and (e) for the case when ΔU_d^s is estimated from the work of Zhao and co-workers.[5]

of φ_s^d, $\Delta U_d^s = -0.00145 + 0.0003 \ln(\varphi_s^d) + 0.00095 \ln(1 - \varphi_s^d)$ nm, also at 184 °C. Budkowski, Steiner, and Klein[12] report $\Delta U_d^s = -0.0016 + 0.00076\varphi_s^d$ nm at 170 °C for this same polymer system.

Thus, the attraction of ends toward the surface U^e is the only unknown needed to apply eq 17 to the data in Figure 3a−e. Rewriting eq 11 as

$$\gamma|_{N^*} \cong \gamma|_\infty + \frac{\rho_b RT(2U^e)}{M_w} \tag{18}$$

it is evident that U^e can be determined from the slope of the surface tension as a function of inverse molecular weight in the limit of infinite molecular weight. It should be noted that due to qualifications mentioned in sections 2.2 and 3.2, the above expression is only suitable for analyzing surface tension data for the higher molecular weight polymers. Here, M_w is the molecular weight of the polymer in kg/mol and ρ_b is the bulk density in kg/m^3. R is the gas constant, and T is the temperature. It is also important to point out that though this expression was derived under the assumption that U^e is purely of entropic origin, it is valid when there is an energetic component to the chain end attraction. In particular, it applies to circumstances where polymer chain ends and midsections are chemically different. When one of the ends is different than the other chemically, as occurs typically when polymers are synthesized anionically, U^e would again represent the arithmetic mean of attraction of ends both the ends of the polymer.

Dee and Sauer[29] made very accurate measurements of surface tension of PS for several polymer molecular weights and at

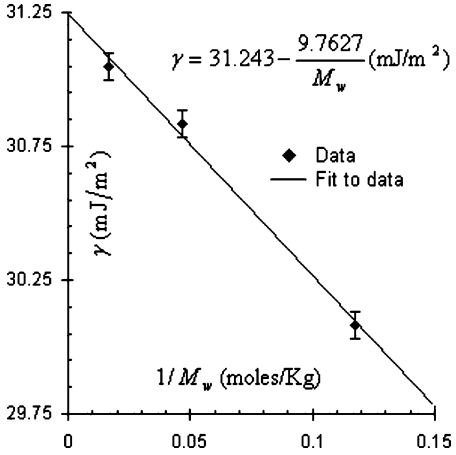

Figure 4. Surface tension of PS as a function its molecular weight at 160 °C. The filled symbols represent data from the work of Dee and Sauer.[29] The line represents a straight line fit to the data. The error bars shown in the figure correspond to experimental errors of 0.05 mJ/m^2.

several temperatures. The PS samples used in their study were anionically initiated with butyllithium and have chemically similar ends to the ones used in the experiments by Hariharan et al. designed to measure the reversal of enrichment.[2] Table II in this reference provides the experimentally measured values of surface tensions at different temperatures and molecular weights. Surface tension values at 160 °C are not directly available. These values have been kindly provided by Dr. Sauer, who obtained them by extrapolating from a full set of temperature-dependent values. Figure 4 illustrates the effect of PS molecular weight on surface tension. Although the number of data points is insufficient for any detailed analysis, it is clear from the figure that the high-molecular-weight results can be well described by a linear function. This analysis allows us to estimate the attraction of chain ends U^e as −1.37 nm for these PS samples. In this calculation ρ_b of PS is taken to be 989 kg/m^3 at 160° C using the parameters of the Sanchez and Lacombe equation of state.[26,30] It is important to note that the estimate of U^e is obtained by disregarding surface tension data for the smallest molecular weight polymers studied by Dee and Sauer. Surface tension data for these polymers do not conform to the linear trend with reciprocal molecular weight observed for their higher molar mass counterparts. Specifically, the molecular weights of the three polymers are 0.5K, 0.7K, and 1.79K, which are at most a few times larger than the molecular weight of a Kuhn unit of polystyrene, 0.72K. This means that coarse graining of surface entropic potentials using Dirac deltas becomes strongly suspect for these materials, and the implicit assumption of random walk chain statistics is likely inappropriate. In comparison, the surface tension data plotted in Figure 4 correspond to PS molecular weights of 8.5, 21.4, and 60 kDa, which correspond to around 12, 30, and 83 Kuhn units. Clearly more surface tension data for linear polystyrenes with molecular weights in the range of 10K to 100K are needed to make firm conclusions about U^e for this polymer. A collaboration between Sauer's group and our group is now underway to remedy this.

Predictions of z_d* using eq 17 and the three parameters determined from independent literature data are compared with the experimental data for PS/dPS blends in Figure 3a−e. Unfortunately, it is not possible to independently determine which of the several literature values of ΔU_d^s is most reliable. As a result, multiple theoretical z_d* plots are provided in each figure. It is evident from these plots that while eq 17 correctly reproduces the experimental trends, the predictions are not quantitative. An important aspect of the experimental results is the presence of a critical crossover PS molecular weight below which a reversal of enrichment is observed. The critical degree of polymerization, $N_h^c = (2U^e/\Delta U_d^s)/[1 + 2U^e/(N_d\Delta U_d^s)]$, at which the reversal is predicted is compared to what is observed experimentally in Table 4. ΔU_d^s values taken from the work of Kumar and Russell[1] yielded the values for N_h^c that are in closest agreement with the observed critical degree of polymerization. This also shows that the theoretical prediction made by Kumar and Russell to obtain the value of ΔU_d^s at 160 °C are consistent with the observed experimental data. It is apparent from Table 4 that the predicted N_h^c values are in reasonably good accord with those deduced from the data. Further, if one takes into account the well-known difficulties in synthesizing clean, narrow molecular weight distribution polymers, of maintaining consistent levels of deuteration in these materials, of accurately measuring and fitting their surface reflectivity profiles, and the paucity of surface tension data for the range of PS molecular weights most suitable for the response analysis, the overall level of agreement between eq 17 and the experimental results in Figure 3a−e can reasonably be described as surprisingly good. The wide range of ΔU_d^s values reported in the literature, nonetheless, indicates that uncertainty in this parameter is likely higher than any of the others and that quantitative agreement between theory and experiment will above all else require more accurate information about ΔU_d^s. It should also be pointed out that a lower value of U^e, as would be obtained for example by including some of the lower molecular weight surface tension data from ref 29, still provides reasonably good predictions of the phenomenon of reversal of enrichment seen by Hariharan et al.[2] Because of the issues discussed above, however, we do not include the lower molecular weight surface tension data in this analysis.

Table 4. Predicted and Actual Crossover Degrees of Polymerization, N_h^c

set (Figure)[a]	predicted[b] N_h^c	experimentally obsd[c] N_h^c
2 (4b)	699	468
4 (4c)	450	580
5 (4d)	699	841
6 (4e)	699	556

[a] Data set corresponding to the original data from the work of Hariharan, Kumar, and Russell[2] and the respective figures here. [b] ΔU_d^s was taken from the work of Kumar and Russell.[1] [c] The observed N_h^c was obtained by fitting a line through the data points.

5. Conclusions

A linear response theory that includes both the energetic and entropic interactions between polymer segments is shown to provide an important tool for studying surface enrichment of polymer and oligomer additives in a host polymer. In particular, we find that this theory predicts reversal of surface enrichment is PS/dPS polymer blends at conditions comparable to where such reversal has been observed experimentally. The critical molecular weight below which the higher surface energy species in the blend is present in excess at the vacuum−blend interface is also predicted reasonably well. A key parameter in this analysis is the attraction of polymer chain ends, U^e, toward the interface. We show that this parameter can be obtained from the initial slope of a plot of surface tension vs reciprocal molecular weight of the pure polymer components. Other parameters in the response theory, e.g. ΔU^s, which represents the energetic driving force and the Flory−Huggins χ parameter of interaction between the blend components, can be found using well-known techniques. Our approach can be generalized to

obtain the entropic driving force for surface segregation of polymeric additives with complex architectures. For these systems it is not just U^e that determines the entropic attraction of chain ends toward the surface, but also U^j, the repulsion of a branched point away from the surface. The parameter U^j is complicated because it also depends on the number of branches that meet at the branched point. Significantly, we show that surface enrichment of a branched additive is determined by the group $n_eU^e + n_jU^j$, which as whole can be determined from independent measurements of the initial slope of surface tension vs the of reciprocal molecular weight.

These results underscore the importance of high-quality surface tension data, particularly at high polymer molecular weights, for polymer migration studies. Our work also points to two new directions—the role of polydispersity on surface tension and migration and the role of higher-order nonlinear terms in the response theory—that are required for quantitative understanding of surface enrichment of additives in polymers. Work underway in the group focuses on improving our current surface tension data set for architecturally complex polymers and on extending the proposed response theory to higher orders, allowing surface migration of oligomeric additives to be accurately predicted.

Acknowledgment. We are grateful to Dr. Bryan B. Sauer for helpful discussions and for providing surface tension data for linear PS. The study was supported by the National Science Foundation (Grants DMR0551185 and DMR 0404278).

Appendix A. Incompressible Lattice Simulations

For the case of a melt of simple linear chains, the relative weight of finding a tail segment of a polymer chain having s segments in lattice layer i, $G[s,i]$, is related to the relative weight of finding a tail segment of chain $s-1$ in size in the neighboring lattice layers by the following iterative equation:[13]

$$G[s,i] = G[1,i](\lambda_1 G[s-1,i-1] + \lambda_0 G[s-1,i] + \lambda_1 G[s-1,i+1]) \quad \text{(A1)}$$

The relative weight of finding a hypothetical free segment of the polymer in any lattice layer i, $G[1,i] = \exp[-u[i]]$, is simply the Boltzmann weight of finding a free unconnected segment of the polymer in any lattice layer. In the case of simulating an infinitely long polymer chain, we have a steady-state expression of (A1):

$$G[\infty,i] = G[1,i](\lambda_1 G[\infty,i-1] + \lambda_0 G[\infty,i] + \lambda_1 G[\infty,i+1]) \quad \text{(A2)}$$

The volume fraction of the segment s belonging to the polymer in a lattice layer i is then obtained as

$$\varphi[s,i] = \varphi[s,\infty]\frac{G[s,i]G[N-s+1,i]}{G[1,i]} \quad \text{(A3)}$$

where $\varphi[s,\infty] = 1/N$ is the volume fraction of segments far away from the surface in the bulk. The incompressibility criterion is satisfied when the contribution of volume fractions of all polymer segments all add up to one, i.e., $\varphi[i] = \sum_{s=1}^{N}\varphi[s,i] = 1$. Here, $\varphi[i]$ is the total volume fraction the polymer in any particular lattice layer. However, if the polymer were infinitely long then all the segments of the polymer are midsection segments composed of two infinitely long tails together. Thus, the volume fraction of such segments $\varphi^\infty[i]$ is then simply $\varphi^\infty[i] = (G[\infty,i])^2/G[1,i]$. At the point of self-consistency $\varphi^\infty[i] = 1$.

For the case of branched polymer melts, we simulated symmetric starlike polymers having p arms. Let N_a be the number of segments in each arm. Then the total number of segments in the starlike polymer N is given by $N = pN_a + 1$, where an extra segment comes from the common segment at the center of star. In our counting notation for the star the first segment of an arm is the end segment of an arm and the (N_a+1)th segment is the common segment at the branch point of the star. In the same way as a linear polymer we first calculate the Boltzmann factors/relative weights of tail segments of simple linear polymer chains of different segments using eq A1. Then, we calculate the Boltzmann factor for a tail segment s of a polymer chain such that at the other end of this chain $p-1$ arms meet. We call this Boltzmann factor $G^{p-1}[s,i]$, where the superscript $p-1$ indicates that at the other end of the chain there is a branch point where $p-1$ arms meet. The Boltzmann factors for tail segments of different ranking indices of the branched polymer chain just described is calculated in the same iterative way as in eq A1:

$$G^{p-1}[s-1,i] = G[1,i](\lambda_1 G^{p-1}[s,i-1] + \lambda_0 G^{p-1}[s,i] + \lambda_1 G^{p-1}[s,i+1]) \quad \text{(A4)}$$

The iterative equation above has the $(s-1)$th factor relating to the sth factor. This is because of our convention of counting the segments in the arm of a star, outside in, and that we first calculate the Boltzmann factor of the tail segment when it is the branch segment. When the tail segment is the branch segment, there is no pth arm and the tail segment is the branch point of a $p-1$ arm star. Thus, its factor is given by

$$G^{p-1}[N_a+1,i] = \frac{(G[N_a+1,i])^{p-1}}{(G[1,i])^{p-2}} \quad \text{(A5)}$$

The numerator is the product of the Boltzmann weights that $p-1$ tail segments belonging to chains of size N_a+1 meet at the same lattice layer, and the denominator accounts for the branch segment being over multiplied $p-2$ times in the numerator as its factor is common to all the $p-1$ arms of the star. The right-hand side of eq A5 is known since the iterative chain eq A1 obtains the numerator and the denominator is the Boltzmann factor of a free segment $G[1,i] = \exp[-u[i]]$. After obtaining the tail segment Boltzmann factors of a simple chain from eq A1 and that of a branched chain through use of eqs A1 and A4 for the starlike polymer, the volume fractions of segments of various ranking indices are obtained as

$$\varphi[s,i] = \varphi[s,\infty]\frac{G[s,i]G^{p-1}[s,i]}{G[1,i]} \quad \text{(A6)}$$

where again $\varphi[s,\infty] = 1/N$ is the volume fraction of that segment far away from the surface in the bulk. The incompressibility criterion is satisfied when the contribution of volume fractions of all polymer segments all add up to one, i.e.

$$\varphi[i] = p(\sum_{s=1}^{N_a}\varphi[s,i]) + \varphi[N_a+1] = 1 \quad \text{(A7)}$$

Here again $\varphi[i]$ is the total volume fraction the polymer in any particular lattice layer. For the boundary conditions at the hard neutral wall, we fix the volume fraction $\varphi[0]$ of the polymer to

be zero in the layer corresponding to the hard neutral wall. This also amounts to setting the Boltzmann factors for tail segments of chains of all sizes and types to be zero at this lattice layer, i.e., $G[s,0] = 0$, and for the star polymer $G^{p-1}[s,0] = 0$ as well. If the number of lattice layers, M, is very large such that it is deep inside the bulk, then it is evident that within a certain number of lattice layers less than M from the vacuum interface, the conditions would approach that of the bulk. As we go deeper into the material, the relative probability of finding any segment of a polymer whether that of a linear or a star approach a same bulk value. This is equivalent to the Boltzmann factor of a tail segment of a chain of any size or type approaching one. In all our simulations it was observed that volume fractions of segments of either polymer approach the bulk value within 4−5 radii of gyration from the vacuum interface. Here in this context of polymer on a cubic lattice the radius of gyration in lattice units of a linear chain is $R_{g,L} = \sqrt{N/6}$, and that of a p-arm symmetric star is $R_{g,S} = \sqrt{(N/6p)(3-2/p)}$.[31] Therefore, we have the second boundary condition as $G[s,m] = 1$ and for the star polymer $G^{p-1}[s,m] = 1$ as well, where m is taken to be the closest integer greater than 5 times the radius of gyration of the polymer. The potentials acting on segments of a polymer and the volume fractions of the segments of the polymer form a self-consistent loop. We start the simulation by assuming an initial volume fraction profile, and then using eq 10, we calculate the self-consistent potentials acting on the segments where we take the Lagrangian parameter as $\alpha'[i] = \zeta(\varphi_1[i] - 1)$. We will comment more about the nature of this assumption of Lagrangian parameter shortly. These potentials would be used to estimate the next volume factions through use of eqs A1−A7 appropriately depending on whether we are simulating a star or a linear polymer, along with boundary conditions. In subsequent iterations, the potentials ($u^{j+1}[i]$) used to calculate the next volume fraction estimates are a combination of the potential estimate ($u^{est}[i]$) due to the volume fraction profile in the current iteration and the potentials used in the immediately ($u^j[i]$) preceding iteration is

$$u^{j+1}[i] = u^j[i] + \eta(u^{est}[i] - u^j[i]) \qquad \text{(A8)}$$

where j is the index denoting the iteration number and η is a relaxation parameter. This iterative procedure is followed until the difference between the potential estimate of the current volume fractions and the potential used to get the current volume fractions $|u^{est}[i] - u^j[i]| \leq 10^{-4}$ to establish self-consistency.

The Lagrangian parameter $\alpha'[i]$ in eq 10 used to ensure incompressibility is taken to be of the form $\alpha'[i] = \zeta(\varphi_1[i] - 1)$, where ζ is some arbitrarily large parameter whose value is normally determined by the ease of convergence of the simulations and the criteria for the incompressibility condition. We have taken this criteria to be $|\varphi[i] - 1| \leq 10^{-3}$ for which we took the value of $\zeta = 1000$.

Similar simulation schemes have been used by other groups for performing self-consistent-field theory simulations in continuum space.[32−34] The value of ζ is typically determined as a compromise between the need for fast convergence and the need to maintain the incompressibility constraint. Larger values of ζ ensure that the incompressibility constraint is more tightly obtained; i.e., for larger values of ζ, at self-consistency the incompressibility expression $(\varphi[i] - 1) < \epsilon$ will have smaller values of ϵ. This becomes clear if one notices that the self-consistent potentials in any lattice layer are of the order of $O[10^{-1}]$, which will be the same order for the expression $\zeta(\varphi[i] - 1)$ occurring in the expression for the self-consistent potential eq 10 through $\alpha'[i] = \zeta(\varphi_1[i] - 1)$. Therefore, at self-consistency$(\varphi[i] - 1) \sim \zeta^{-1}O[10^{-1}]$. At a value of $\zeta = 1000$, we should get $(\varphi[i] - 1) \sim O[10^{-4}]$, which is precisely what is observed.

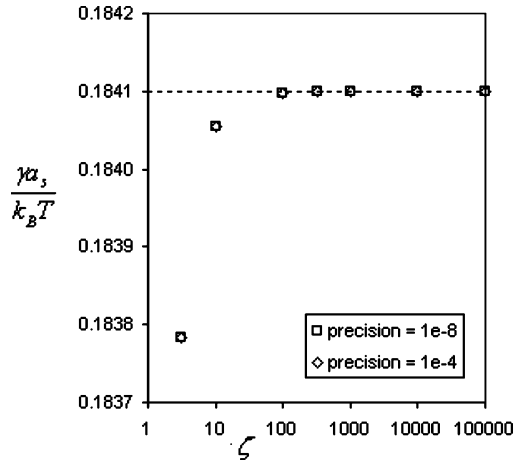

Figure 5. Surface tension, $\gamma a_s/k_BT$, of a 2001 degree of polymerization linear polymer as a function of parameter ζ. Square represent the simulation data for a precision of 10^{-8} and diamonds for a precision of 10^{-4}.

To determine the effect of ζ on the accuracy of our simulations, Figure 5 plots dimensionless surface tension $\gamma a_s/k_BT$ obtained from simulations performed at variable ζ. The figure shows that the surface tension increases monotonically and beyond $\zeta \sim 100$ asymptotically approaches a value of around 0.184. Figure 5 also shows the effect of numerical precision or convergence criterion, $|u^{est}[i] - u^j[i]| \leq 10^{-4}$ to $|u^{est}[i] - u^j[i]| \leq 10^{-8}$. Again, beyond $\zeta \sim 100$ an asymptote is seen, meaning that the choice $\zeta \sim 1000$ is satisfactory.

To execute these simulations, we assume an initial volume fraction profile $\varphi[i] = 1$ in all lattice layers. The Lagrangian parameter, $\alpha'[i] = \zeta(\varphi_1[i] - 1)$, is obtained in subsequent steps from changes in the species volume fraction. For large values of the parameter ζ the previous order of magnitude analysis shows $(\varphi[i] - 1) \sim \zeta^{-1}O[10^{-1}]$. Therefore, at the point of self-consistency $|u^{est}[i] - u^j[i]| \leq 10^{-4}$, the incompressibility criterion is strongly enforced.

Appendix B. Compressible Lattice Simulations

The compressible lattice simulations are similar to the incompressible lattice simulations as described in Appendix A. However, because of the presence of voids in the system as the second component, the Lagrangian parameter which was introduced to maintain the space-filling constraint can be eliminated, so that the potential that a segment of a polymer in lattice layer i can be written as[13]

$$u[i] = -2\chi_v(\langle\varphi[i]\rangle - \varphi_b) - \ln\left[\frac{1-\varphi[i]}{1-\varphi_b}\right] \qquad \text{(B1)}$$

The propagators are calculated for the linear and symmetric star ends in the same manner as the case of the incompressible lattice simulations, i.e., through the use of eqs A1−A7. The bulk volume fractions φ_b, which are needed in eqs A3 and A6, are calculated from the Sanchez and Lacombe equation of state eq 14. Therefore, $\varphi[s,\infty] = \varphi_b/N^*$. For the case of an infinitely long polymer, the steady-state propagator equation is same as in eq A2. The volume fraction of segments $\varphi^\infty[i]$ belonging to this infinitely long polymer is then taken as $\varphi^\infty[i] = \varphi_b^\infty$-

$(G[\infty,i])^2/G[1,i]$, where φ_b^∞ is evaluated according to the conditions of the simulation described in section 3.2 and through eq 14 taking $N^* = \infty$.

The boundary conditions and the criteria for the iterative scheme for the attainment of self-consistency are the same as described in Appendix A for incompressible lattice simulations. The iterative scheme was stopped once $|u^{est}[i] - u^j[i]| \leq 10^{-8}$.

References and Notes

(1) Kumar, S. K.; Russell, T. P. *Macromolecules* **1991**, *24*, 3816−3820.
(2) Hariharan, A.; Kumar, S. K.; Russell, T. P. *J. Chem. Phys.* **1993**, *98*, 4163−4173.
(3) Jones, R. A. L.; Kramer, E. J.; Rafailovich, M. H.; Sokolov, J.; Schwarz, S. A. *Phys. Rev. Lett.* **1989**, *62*, 280−283.
(4) Norton, L. J.; Kramer, E. J.; Bates, F. S.; Gehlsen, M. D.; Jones, R. A. L.; Karim, A.; Felcher, G. P.; Kleb, R. *Macromolecules* **1995**, *28*, 8621−8628.
(5) Zhao, X.; Zhao, W.; Sokolov, J.; Rafailovich, M. H.; Schwarz, S. A.; Wilkens, B. J.; Jones, R. A. L.; Kramer, E. J. *Macromolecules* **1991**, *24*, 5991−5996.
(6) Minnikanti, V. S.; Archer, L. A. *J. Chem. Phys.* **2005**, *123*, 144902-(1)−144902(9).
(7) Walton, D. G.; Mayes, A. M. *Phys. Rev. E* **1996**, *54*, 2811−2815.
(8) Foster, M. D.; Greenberg, C. C.; Teale, D. M.; Turner, C. M.; Corona-Galvan, S.; Cloutet, E.; Butler, P. D.; Hammouda, B.; Quirk, R. P. *Macromol. Symp.* **2000**, *149*, 263−268.
(9) Budkowski, A. *Adv. Polym. Sci.* **1999**, *148*, 1−111.
(10) Schmidt, I.; Binder, K. *J. Phys. (Paris)* **1985**, *46*, 1631−1644.
(11) Shull, K. R. *Macromolecules* **1992**, *25*, 2122−2133.
(12) Budkowski, A.; Steiner, U.; Klein, J. *J. Chem. Phys.* **1992**, *97*, 5229−5238.
(13) Fleer, G. J.; Stuart, M. A. C.; Scheutjens, J. M. H. M.; Cosgrove, T.; Vincent, B. *Polymers at Interfaces*, 1st ed.; Chapman and Hill: London, 1993.
(14) Wu, D. T.; Fredrickson, G. H.; Carton, J.-P.; Ajdari, A.; Leibler, L. *J. Polym. Sci., Part B: Polym. Phys.* **1995**, *33*, 2373−2389.
(15) Wu, D. T.; Fredrickson, G. H. *Macromolecules* **1996**, *29*, 7919−7930.
(16) Minnikanti, V. S.; Archer, L. A. *J. Chem. Phys.* **2005**, *122*, 084904-(1)− 084904(11).
(17) de Gennes, P.-G. *Scaling Concepts in Polymer Physics*; Cornell University Press: Ithaca, NY, 1979.
(18) Leibler, L. *Macromolecules* **1980**, *13*, 1602−1617.
(19) Theodorou, D. N. *Macromolecules* **1988**, *21*, 1400−1410.
(20) Kumar, S. K.; Jones, R. L. *Phys. Rev. Lett.* **2001**, *87*, 179601-1.
(21) Kumar, S. K.; Jones, R. L. *Adv. Colloid Interface Sci.* **2001**, *94*, 33−38.
(22) Theodorou, D. N. *Macromolecules* **1989**, *22*, 4578−4589.
(23) Hariharan, A.; Kumar, S. K.; Russell, T. P. *J. Chem. Phys.* **1993**, *98*, 6516−6525; **1993**, *99*, 4041−4050.
(24) Tang, H.; Freed, K. F. *J. Chem. Phys.* **1991**, *94*, 1572−1583.
(25) Sanchez, I. C.; Lacombe, R. H. *J. Phys. Chem.* **1976**, *80*, 2352−2362.
(26) Poser, C. I.; Sanchez, I. C. *J. Colloid Interface Sci.* **1979**, *69*, 539−548.
(27) Roe, B. P. *Probability and Statistics in Experimental Physics*, 3rd printing; Springer-Verlag: New York, 1998.
(28) Bates, F. S.; Wignall, G. D. *Phys. Rev. Lett.* **1986**, *57*, 1429−1432.
(29) Dee, G. T.; Sauer, B. B. *J. Colloid Interface Sci.* **1992**, *152*, 85−103.
(30) Brandrup, J.; Immergut, E. H. *Polymer Handbook*, 3rd ed.; John Wiley and Sons: New York, 1989.
(31) Rubinstein, M.; Colby, R. H. *Polymer Physics*; Oxford University Press: New York, 2003.
(32) Genzer, J.; Faldi, A.; Oslanec, R.; Composto, R. J. *Macromolecules* **1996**, *29*, 5438−5445.
(33) Shull, K. R.; Kramer, E. J. *Macromolecules* **1990**, *23*, 4769−4779.
(34) Donley, J. P.; Fredrickson, G. H. *J. Polym. Sci., Part B: Polym. Phys.* **1995**, *33*, 1343−1350.

MA061377D